Biochemical Pharmacology xxx (xxxx) xxx–xxx

Contents lists available at ScienceDirect

Biochemical Pharmacology

journal homepage: www.elsevier.com/locate/biochempharm

A novel combination of astilbin and low-dose methotrexate respectively targeting A_{2A}AR and its ligand adenosine for the treatment of collagen-induced arthritis

Yuxiang Ma[1], Zhe Gao[1], Fang Xu, Li Liu, Qiong Luo, Yan Shen, Xuefeng Wu, Xingxin Wu, Yang Sun, Xudong Wu*, Qiang Xu*

State Key Laboratory of Pharmaceutical Biotechnology, School of Life Sciences, Nanjing University, 163 Xianlin Avenue, Nanjing 210023, China

ARTICLE INFO

Keywords:
Rheumatoid arthritis
MTX combination therapy
Adenosine
A_{2A}AR
Astilbin

ABSTRACT

Methotrexate (MTX) is widely used for rheumatoid arthritis (RA) treatment with frequently serious adverse effects. Therefore, combination of low-dose MTX with other drugs is often used in clinic. In this study, we investigated the improvement of astilbin and low-dose MTX combination on collagen-induced arthritis in DBA/1J mice. Results showed that the clinic score, incidence rate, paw swelling, pathological changes of joints and rheumatoid factors were more alleviated in combination therapy than MTX or astilbin alone group. Elevated antibodies (IgG, IgG1, IgG2a, IgM and anti-collagen IgG) and pro-inflammatory cytokines (IL-1β, IL-6, TNF-α, IFN-γ and IL-17A) in serum were significantly inhibited, while anti-inflammatory cytokine, IL-10, was enhanced by combination therapy. Further studies indicated that combination therapy significantly decreased Th1 and Th17 cell differentiation and increased Treg cell differentiation. Mechanisms analysis demonstrated combination therapy greatly inhibited Con A-activated MAPK and inflammatory transcriptional signals. Moreover, MTX activated adenosine release and astilbin specifically up-regulated A_{2A} adenosine receptor (A_{2A}AR) expression simultaneously, which most probably contributed to the synergistic efficacy of combination therapy. ZM241385, a specific antagonist of A_{2A}AR, greatly blocked the effects of combination therapy on T cell functions and downstream pathways. All these findings suggest that astilbin is a valuable candidate for low-dose MTX combined therapy in RA via increasing A_{2A}AR/adenosine system and decreasing ERK/NFκB/STATs signals.

1. Introduction

Rheumatoid arthritis (RA) is characterized as activating many inflammatory pathways that finally lead to cartilage destruction and bony erosions. The conventional treatment of RA includes disease-modifying antirheumatic drugs (DMARDs), nonsteroidal anti-inflammatory drugs (NSAIDs) and corticosteroids. In the management of early and established RA, MTX is recommended as the first-line drug by the European League Against Rheumatism (EULAR) and the American College of Rheumatology (ACR). However, as an anti-metabolic agent, MTX may cause serious adverse events such as cytopenia, serious infections, liver damage [1–5], mucocutaneous problems and hypersensitivity pneumonitis [6]. Therefore, the clinic application of MTX in RA is limited, and combination with other medications are often used in order to reduce side effects [4,7]. However, while receiving low-dose MTX owing to its side effects, patients with active RA exhibit an incomplete response or flare of disease activity [8]. Therefore, we hope to find novel DMARDs to make patients complete response to low-dose MTX in combination therapy.

In our previous study, astilbin, the flavonoid compound isolated from *Rhizoma Smilacis Glabrae*, shows strong immunomodulatory activity without any obvious toxicity [9–13]. Huang has reported that astilbin exhibits the anti-inflammatory activity in macrophage [14]. Especially, we have found that astilbin can alleviate collagen-induced arthritis (CIA) in Kunming mice via suppressing MMP and NO production of lymphocytes [10]. Other researchers also reported that

Abbreviations: RA, rheumatoid arthritis; DMARDs, disease-modifying antirheumatic drugs; ACR, American College of Rheumatology; MPO, Myeloperoxidase; CIA, collagen-induced arthritis; MMP3, matrix metalloproteinase 3; MCP-1, Monocyte chemoattractant protein-1; RANKL, receptor activator for nuclear factor-κB ligand; AR, adenosine receptor; A_1AR, A_1 adenosine receptor; A_{2A}AR, A_{2A} adenosine receptor; A_{2B}AR, A_{2B} adenosine receptor; A_3AR, A_3 adenosine receptor; Con A, Concanavalin A; PMA, Phorbol-12-myristate-13-acetate; ERK, extracellular regulated protein kinases; NFκB, nuclear transcription factor-κB; STATs, Signal transducers and activators of transcription

* Corresponding author.
E-mail addresses: xudongwu@nju.edu.cn (X. Wu), molpharm@163.com (Q. Xu).
[1] These authors are contributed equally to this work.

https://doi.org/10.1016/j.bcp.2018.01.033
Received 26 November 2017; Accepted 18 January 2018
0006-2952/

astilbin attenuated complete freund's adjuvant-induced arthritis in rats [15]. Here, we continue to study the potential of astilbin and low-dose MTX combination therapy and the underlying mechanism of astilbin in complement effects.

Th1 and Th17 cells are pro-inflammatory phenotypes of $CD4^+$ T cells by secreting IFN-γ and IL-17A, respectively. While, Th2 and Treg cells are anti-inflammatory phenotypes through generating IL-4 and IL-10. MTX and other DMARDs ameliorates RA is partially owing to their capability to reverse Th1/Th2, Th17/Treg imbalance [16,17]. Therefore, T cell differentiation is the central event for RA therapy.

Furthermore, MTX is reported to exert the anti-inflammatory effects by promoting the release of endogenous anti-inflammatory mediator, adenosine [18,19]. Adenosine is a purine nucleoside that binds four specific adenosine receptors, A_1AR, $A_{2A}AR$, $A_{2B}AR$ and A_3AR [19]. Different receptors exert diverse effects in immunoregulation, and $A_{2A}AR$ and A_3AR are more important in RA progression [20]. As ligand and receptor system, adenosine and its receptors supply the possibilities to seek appropriate drug combination for RA treatment.

In this study, we first reveal that combination therapy of astilbin and low-dose MTX is more efficient than single use in RA, without obvious toxic effects. Further mechanism study demonstrates that astilbin and low-dose MTX regulates T cells functions via adenosine release and $A_{2A}AR$ expression respectively, which is different from other MTX combination medicine.

2. Materials and methods

2.1. Animals

Specific-pathogen-free, eight-week-old male DBA/1J mice were purchased from the Shanghai Experimental Animal Center, the Chinese Academy of Sciences. Eight-week-old C57BL/6 mice were purchased from Model Animal Genetics Research Center of Nanjing University (Nanjing, China). They were maintained with free access to pellet food and water in plastic cages at 21 ± 2 °C and kept on a 12 h light-dark cycle. Animal welfare and experimental were carried out strictly in accordance with the Guide for the Care and Use of Laboratory Animals (Ministry of Science and Technology of China, 2006) and the related ethical regulations of our university. All efforts were made to minimize animals' suffering and to reduce the number of animals used.

2.2. Reagents and antibodies

Astilbin, 3, 3, 4′, 5, 7-pentahydroxyflavanone 3–6[-deoxy-([alpha]-L-mannopyranoside)], was isolated from the rhizome of *Smilax glabra* and purified in our laboratory as previously described [21]. The purity was determined by HPLC to be above 99%. Bovine type II collagen (CII) and complete freund's adjuvant (CFA) were purchased from Chondrex (WA, USA). Concanavalin A (Con A), MTT, MTX, incomplete freund's adjuvant (IFA) phorbol 12-myristate13-aceate (PMA) and ionomycin were obtained from Sigma (MO, USA). ZM241385 and SCH772984 were from Selleck Chemicals (Texas, USA). Mouse anti-CD25-APC, mouse anti-CD4-FITC, mouse anti-IFN-γ-PE, mouse anti-IL-4-APC, mouse anti-IL-17A-APC and mouse anti-Foxp3-PE were from ebioscience Inc. (CA, USA).TNF-α, IFN-γ, IL-1β, IL-2, IL-4, IL-6, IL-10, IL-17A Elisa kits were from Dakewe Biotech Co., Ltd. (Beijing, China). IgG, IgG1, IgG2a, IgG2b and IgM ELISA kit was from Bai Aotong Experimental Materials Center (Luoyang, China). Recombinant murine IL-12, IL-4, IL-6 and TGF-β were purchased from PeproTech (NJ, USA). Fetal bovine serum (FBS), RPMI 1640, penicillin, streptomycin, phosphate buffered saline (PBS) and 0.25% trypsin, protease inhibitor cocktail, BCA™ protein assay kit were purchased from Thermo Fisher Scientific Inc. (MA, USA). WB/IP lysate buffer were purchased from Beyotime Biotechnology (Shanghai, China). a polyvinylidene difluoride membrane were from Millipore (MA, USA) Monensin and Cytometric bead array (CBA) cytokine assay kit was purchased from BD Biosciences (CA, USA). The Real Envision Detection kit was purchased from Gene Tech (Shanghai, China). The antibodies used in this study were as follows: MCP-1, MMP3, RANKL, OB-cadherin, STAT1 and STAT6 were purchased from Santa Cruz Biotechnology (CA, USA); p-ERK, ERK, p-P38, P38, p-JNK, JNK, p-STAT1, p-STAT3, STAT3 and p-STAT6 were purchased from Cell Signaling Technology (MA, USA); Anti-Adenosine Receptor A2a antibody was from Abcam company (MA, USA). Anti-β-actin was from Abmart (Shanghai, China).

2.3. Induction and assessment of collagen-induced arthritis (CIA) and drug administration

Eight-week-old male DBA/1J mice were immunized on day 0, at the base of the tail, with an intradermal injection of 100 μg CII emulsified in CFA. On day 21, mice were boosted with an injection of 100 μg CII dissolved in IFA. Mice were examined daily and scored for arthritis severity, with each paw assigned a clinical score as follows: 0, no swelling or redness; 1, swelling or redness in one joint; 2, involvement of > 2 joints; and 3, severe arthritis affecting all paws and joints (maximum score = 12). According to our previous results, treatment with 10 mg/kg methotrexate showed excellent antirheumatic properties, but with severe adverse events [22]. In this case, we chose 1.5 mg/kg methotrexate which could be well tolerated and 5, 10 or 20 mg/kg astilbin for combination therapy. From day 21, for treatment, astilbin in 0.5% methylcellulose was administered intragastrically (i.g.) at 5, 10, or 20 mg/kg/d; MTX in 0.5% methylcellulose was administered i.g. at 1.5 mg/kg/2d; combination of astilbin and MTX was administered i.g. at the same dose as single use. Vehicle was administered i.g with 0.5% methylcellulose only. On day 42, all the mice were sacrificed.

2.4. Cell culture

Mouse splenocytes or T cells isolated from mice were cultured in RPMI 1640 medium supplemented with 10% FBS, 100 U/ml penicillin, and 100 μg/ml streptomycin at 37 °C in a 5% (v/v) humidified CO_2 incubator.

2.5. Splenocyte purification and intracellular staining of cytokines

Mouse splenocytes were isolated from spleen of every group of DBA/1J mice on the day 42 post immunization. Cells were stimulated for 4 h with PMA (50 ng /ml) and ionomycin (1 μg/ ml) and a protein-transport inhibitor containing monensin before detection by staining with antibodies. Surface markers were stained for 15–20 min in room temperature in PBS with 1% FCS, then were fixed in Cytofix and permeabilized with Perm/Wash Buffer using Fixation Permeabilization Solution kit (BD Biosciences, CA, USA) and stained anti-IFN-γ-PE, anti-IL-4-APC, anti-IL-17A-APC, anti-Foxp3-PE antibody diluted in Perm/Wash buffer as described [23]. The cells were analyzed by flow cytometry using a FACSVerse (BD Biosciences).

2.6. T Cells isolation and $CD4^+$ T-cell differentiation in vitro

$CD4^+$ T cells and naive T cells from spleen and lymph node were isolated from C57BL/6 mice using $CD4^+$T cell isolation kit and $CD4^+CD62^+$ naive T cell isolation kit from Miltenyi Biotec (CA, USA), according to the manufacturer's instructions. For activation, $CD4^+$ T cells were stimulated with Con A (1 μM) for 24 h. For Th1, Th2 and Th17 differentiation, naive T cells were incubated with plate-bound mAbs of anti-CD3 and anti-CD28 in the presence of ThN condition (non-skewing cytokines), Th1 condition (10 ng/ml IL-12 and 5 μg/ml anti-IL-4 mAb), Th2 condition (10 ng/ml IL-4, 5 μg/ml anti-IFN-γ mAb and 5 μg/ml anti-IL-12 mAb), Th17 condition (20 ng/ml IL-6, 1 ng/ml recombinant human (rh) TGF-β1, 5 μg/ml anti-IFN-γ mAb and 5 μg/ml anti-IL-4 mAb) or Treg condition (1 ng/ml rhTGFβ1 and 60 IU/ml IL-2) for 4 days.

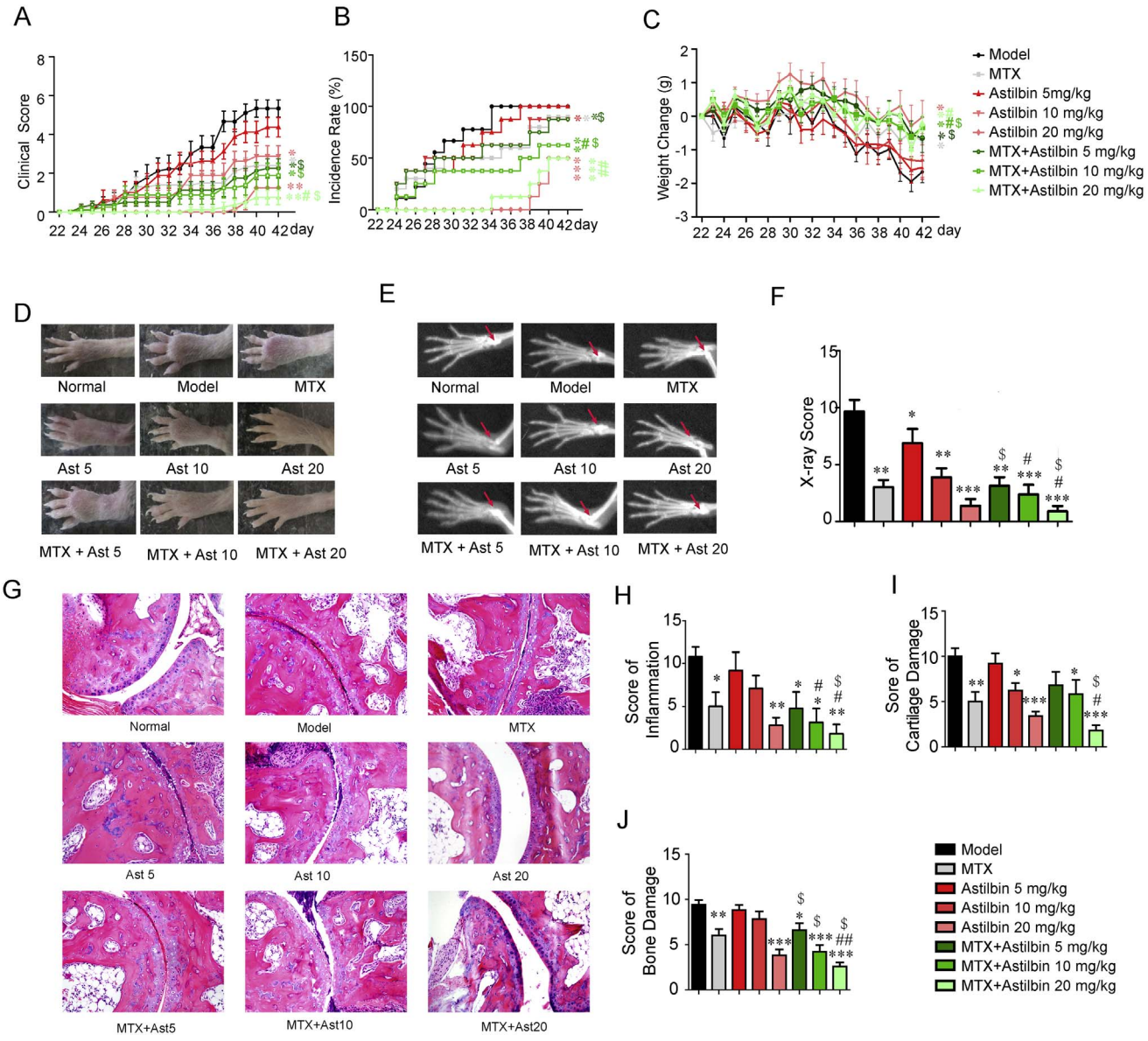

Fig. 1. Combination of astilbin and low-dose of MTX alleviates symptoms of CIA in DBA/1J mice. (A) The arthritis clinical scores of CIA. (B) Incidence of arthritis. (C) Body weight change. (D) Representative photographs of hindpaws from each group. (E and F) Radiographs of representative hindpaws of the CIA mice, and score of radiographs. (G–J) Arthritic joints from CIA mice were harvested on day 42 post immunization. Joints sections were stained by H&E (200×). Representative images (G), inflammatory infiltration scores (H), cartilage damage (I) and bone damage (J) were shown. Error bars are means ± SEM of each CIA group (n ≥ 8). $^{*}P \leq 0.05$, $^{**}P \leq 0.01$, $^{***}P \leq 0.001$ versus model (black histogram). $^{\#}P \leq 0.05$, $^{\#\#}P \leq 0.01$ versus MTX alone (grey histogram). $^{\$}P \leq 0.05$ versus corresponding astilbin alone (red histogram).

2.7. Measurement of cytokines, IgG, IgG1, IgG2a, IgG2b and IgM

Serum was collected from every group of DBA/1J mice on the day 42 post immunization. The content of IL-2, IL-6, IL-4, IL-10, IL-17A, TNF-α and IFN-γ cytokines in serum was measured by CBA cytokine assay kit, according to the manufacturer's instruction. Serum IL-1β, IgG, IgG1, IgG2a, IgG2b and IgM content was measured by ELISA kits, according to the manufacturer's instruction.

Splenocytes obtained from spleen of every group of DBA/1J mice 42 days after immunization were cultured with Con A (1 μM) for 48 h and supernatants were collected. T cells isolation and activation was the same as above description in 2.6, and treated with different drugs as description in corresponding figure legends. Supernatants were collected. Cytokines measurement was measured by ELISA kits.

2.8. Analysis of anti-CII IgG antibody production

Serum samples were collected on day 42 after post-immunization, and the anti-CII IgG titer was measured using ELISA. Briefly, ELISA microtiter plates (Termo Fisher Scientific) were coated with CII (10 μg/ml in PBS) at 4 °C overnight, followed by a blocking step with 3% bovine serum albumin (BSA) in Tris bufer for 1 h at room temperature. Tested sera were then serially diluted in Tris-bufered saline (pH, 8.0) containing 1% BSA and 0.5% tween-20 and added to a well at 4 °C overnight. After washing for five to seven times, bounded IgG was detected using an HRP-conjugated sheep anti-mouse IgG as secondary antibodies (Abs). After washing, the plate was developed using ABTS (Roche Diagnostic Systems) as a substrate, and the reaction was stopped with H_2SO_4. The optical density (OD) was determined at 450 nm with an ELISA reader (Tecan Sunrise).

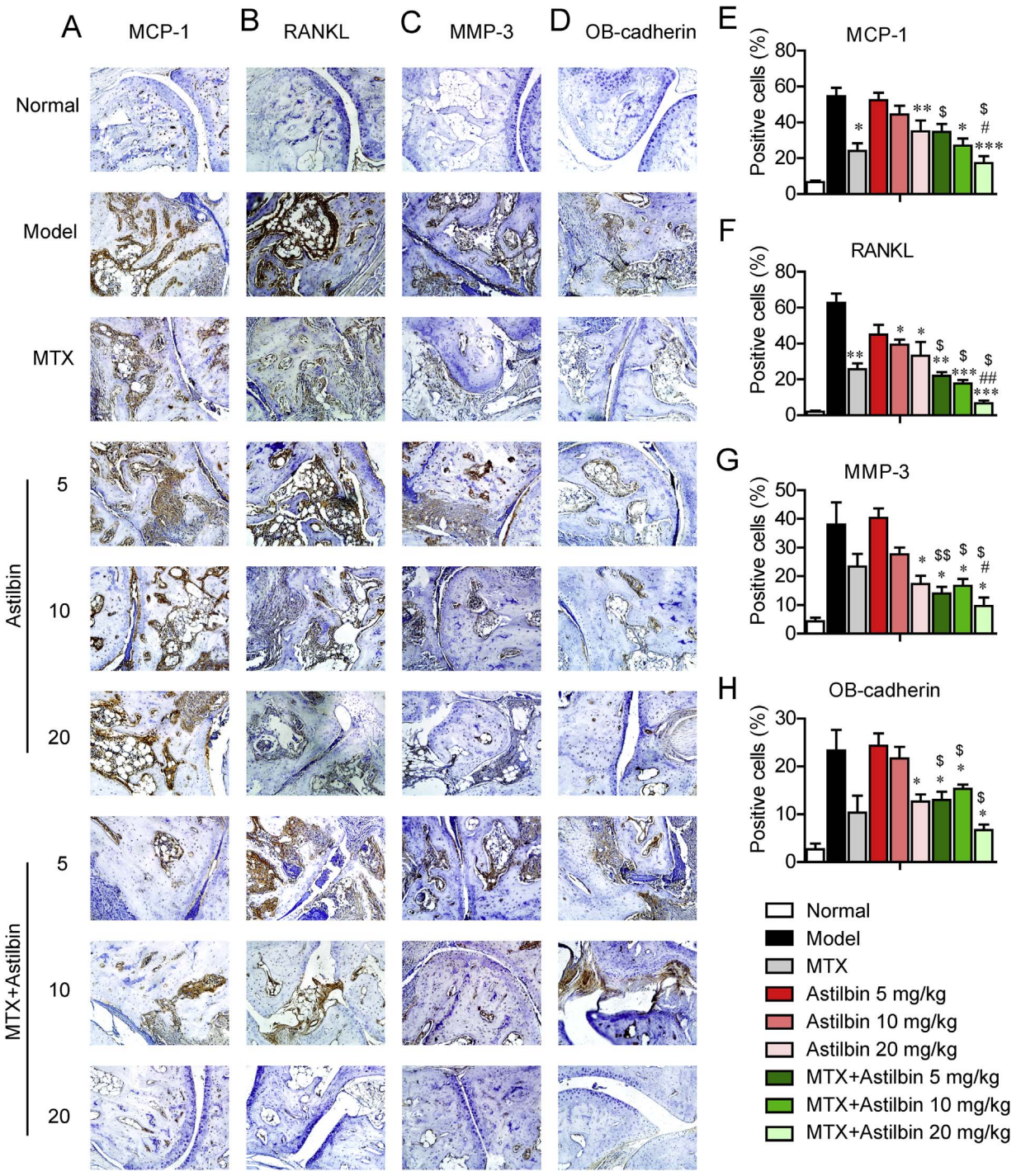

Fig. 2. Combination therapy decreases the expression of pro-inflammatory factors in joints. Hindpaw sections obtained from each group of mice with CIA on day 42 post immunization were stained with (A) anti-MCP-1, (B) anti-RANKL, (C) anti-MMP3, (D) anti-OB-cadherin in an immunohistochemical (IHC) assay (200×). Representative images of IHC were shown. (E–H) Corresponding quantification of positive cells was shown. $^{*}P \leq 0.05$, $^{**}P \leq 0.01$, $^{***}P \leq 0.001$ versus model (black histogram). $^{\#}P \leq 0.05$, $^{\#\#}P \leq 0.01$ versus MTX alone (grey histogram). $^{\$}P \leq 0.05$, $^{\$\$}P \leq 0.05$ versus corresponding astilbin alone (red histogram).

2.9. Western blotting

Harvested cells were lysed in WB/IP lysate buffer containing protease inhibitor cocktail. Total extracted proteins were determined by BCA™ protein assay kit. Equal amounts of protein lysates were separated by 10% SDS-PAGE and subsequently electrotransferred by Electrophoresis and Blotting Apparatus (Bio-Rad, CA, USA) onto polyvinylidene difluoride membranes. Following, the membranes were blocked with 5% nonfat milk for 1 h at room temperature. The blocked membrane was incubated with the indicated primary antibodies, and then with a horseradish peroxidase-conjugated secondary antibody. Finally, Protein bands were visualized using the Western blotting detection system according to the manufacturer's instructions (Cell Signaling Technology, MA, USA). The denaitometric analysis was conducted via the software Quantity One-4.6.5 (Bio-Rad Laboratories, CA, USA).

2.10. Real-time PCR (RT-PCR)

Total RNA was extracted from the cells with trizol reagent and

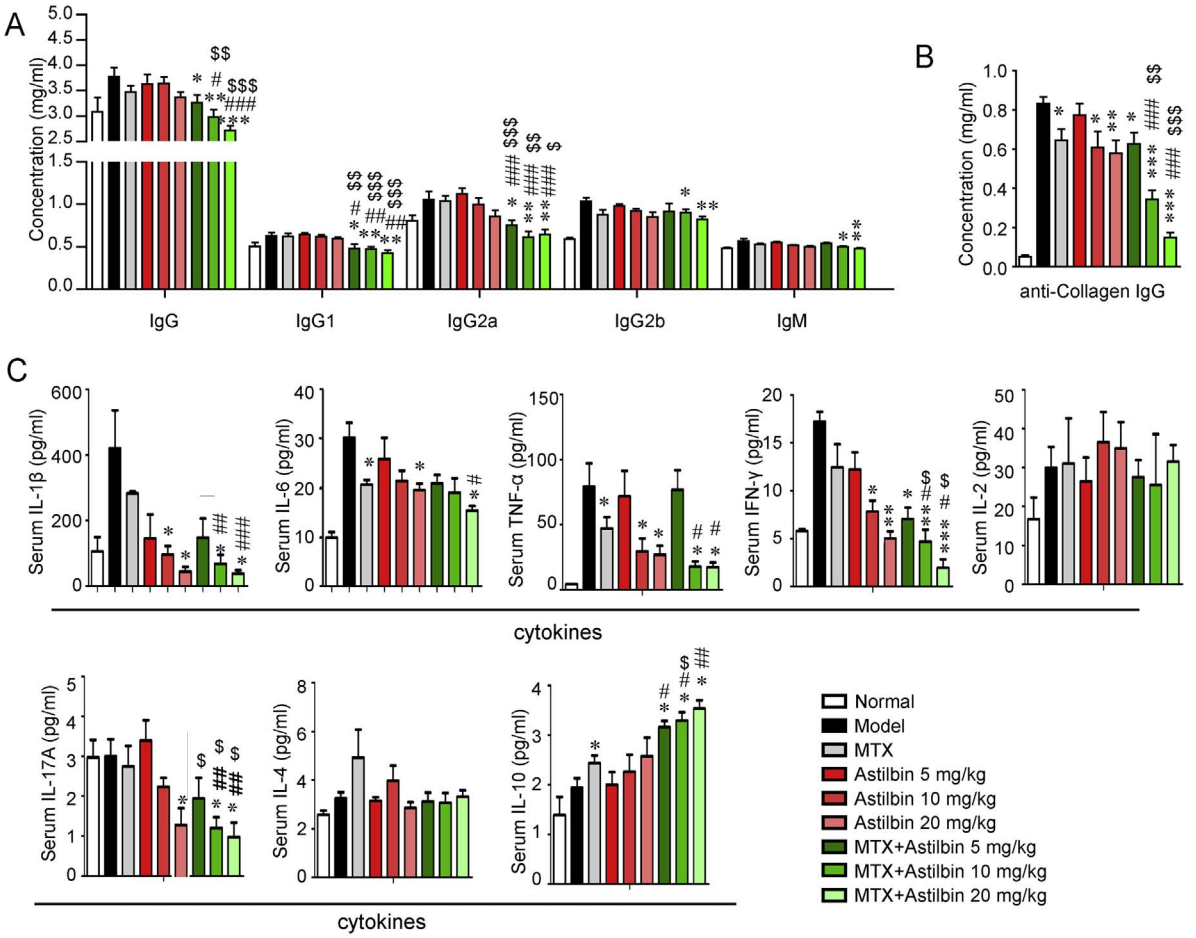

Fig. 3. Combination therapy reduces the levels of inflammation-related antibodies and cytokines in serum. The serum was collected on day 42 post immunization from each CIA group. (A) Levels of total IgG and isotype-specific IgG1, IgG2a, IgG2b, and levels of IgM were detected by specific ELISA kit. (B) Anti-Collagen IgG level in serum was assessed by ELISA. (C) Cytokines (IL-2, IL-4, IL-6, IL-10, IL17A, TNF-α, IFN-γ) in the serum were measured by CBA assay. Error bars are means ± SEM of each CIA group ($n \geq 8$). $^{*}P \leq 0.05$, $^{**}P \leq 0.01$, versus model (black histogram). $^{\#}P \leq 0.05$, $^{\#\#}P \leq 0.01$ versus MTX alone (grey histogram). $^{\$}P \leq 0.05$ versus corresponding astilbin alone (red histogram).

reversed to cDNA and subjected to quantitative PCR, which was performed with the BioRad CFX96 Touch™ Real-Time PCR Detection System (BioRad, CA, USA) using iQTMSYBR®Green Supermix. And threshold cycle numbers were obtained using BioRad CFX Manager Software. The program was described as following: 1 cycle of 95 °C for 2 min, and 40 cycles of 95 °C for 10 s, 60 °C for 30 s, and 72 °C for 30 s. The primer sequences used in this study were: *Adora1a,* 5′-TGTGCCC GGAAATGTACTGG-3′ (forward) and 5′-TCTGTGGCCCAATGTTGAT AAG-3′(reverse); *Adora2a*, 5′-GCCATCCCATTCGCCATCA-3′ (forward) and 5′-GCAATAGCCAAGAGGCTGAAGA-3′ (reverse); *Adora2b*, 5′- AGC TAGAGACGCAAGACGC-3′ (forward) and 5′- GTGGGGGTCTGTAATG CAC-3′ (reverse); *Adora3a*, 5′- AAGGTGAAATCAGGTGTTGAGC-3′ (forward), and 5′- AGGCAATAATGTTGCACGAGT-3′ (reverse).

2.11. Histopathology

Paws for histological analysis were removed from mice and immediately fixed in 4% paraformaldehyde. The paws were decalcified in EDTA, embeded in paraffin, sectioned, and stained with H&E. The sections were scored to assess joint inflammation, on a scale of 0–4 under blinded conditions, according to the degree of hyperplasia in the synovial lining, mononuclear cell infiltration, and pannus formation. Cartilage damage was graded as: 1, normal appearance; 2, mild articular cartilage damage; 3, moderate cartilage damage with abnormal formations consisting of dead chondrocytes (abnormal osteochondrodysplasia); 4, joint ankylosis, complete loss of cartilage, and marked osteochondrodysplasia. For bone resorption grading: 1, normal appearance; 2, bone resorption at the bone margins; 3, bone resorption involving the subchondral bone but sparing the cartilage and bone interface; 4, marked bone resorption involving the cartilage and bone interface. The score for each mouse was the sum of the scores for the four limbs. (maximum score = 16).

2.12. Immunohistochemistry

Deparaffinized joint sections were subjected to Ag retrieval in 0.01 M citrate buffer solution. After blocking endogenous peroxidase activity in 3% H_2O_2, the sections were incubated with anti-MMP3 mAb, anti-RANKL mAb, anti-MCP-1 mAb, anti-OB-cadherin mAb, or normal mouse IgG overnight at 4 °C. Then the sections were rinsed and visualized by immunoperoxidase staining with a Real Envision Detection kit, according to the manufacturer's instructions.

2.13. Radiological examinations

At day 42, all the DBA/1J mice were anesthetized and radiographs of the hind paws were obtained with a lumina XR system (Caliper IVIS Spectrum) before sacrifice. Images were read independently in a blinded fashion, and radiologic score was assessed according to the following criteria: 0) no radiologic changes were observed; 1) mild changes, with tissue swelling and edema; 2) moderate changes, with joint erosion and disfiguration; and 3) severe changes, with bone erosion and osteophyte formation. The total radiologic scores were calculated from the sum of four paws of each mouse; the maximum value

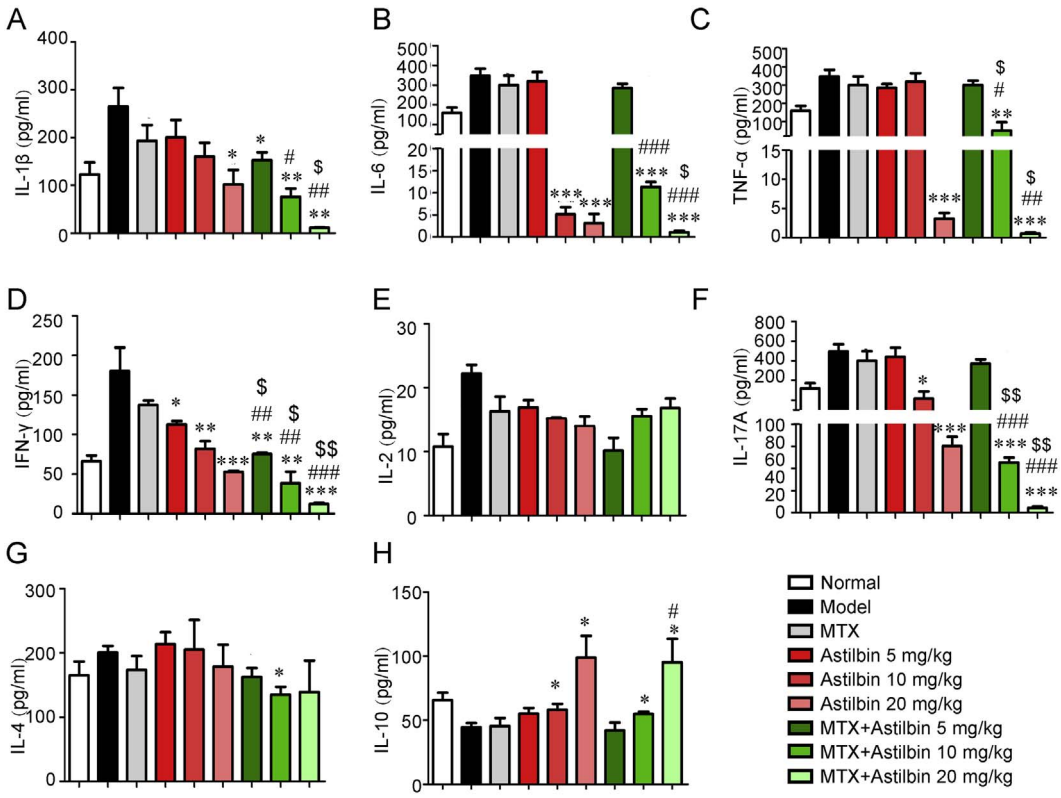

Fig. 4. Combination therapy induces a shift in systemic cytokine profiles from pro-inflammation to anti-inflammation. Splenocytes obtained from DBA/1 mice 42 days after immunization were cultured with Con A for 48 h. Supernatants were collected and analyzed for cytokine production by ELISA kits. (A-H) Levels of IL-1β, IL-6, TNF-α, IFN-γ, IL-17A, IL-2, IL-10, IL-4. $^{*}P \leq 0.05$, $^{**}P \leq 0.01$, $^{***}P \leq 0.001$ versus model (black histogram). $^{\#}P \leq 0.05$, $^{\#\#}P \leq 0.01$, $^{\#\#\#}P \leq 0.01$ versus MTX alone (grey histogram). $^{\$}P \leq 0.05$ versus corresponding astilbin alone (red histogram).

was 12.

2.14. Adenosine analysis

Serum was obtained from every group of DBA/1J mice on the day 42 post immunization. T cells isolated from C57BL/6 mice were treated with MTX (0.1 μM), astilbin (3, 10, 50 μM) or combination of them, and then stimulated by Con A (1 μM) for 24 h. Adenosine concentration in serum and T cells was measured by HPLC as previously described[24], with simple modification. In brief, 100 μl serum or T cells of three mice was added to 100 μl 0.6 M cold perchloric acid on ice, vortexed, and subsequently sonicated for 10 s with output 6. The homogenate was centrifuged at 12,000 × g for 10 min at 4 °C. The supernatant (113 μl) was transferred to a new tube and neutralized with 8.2 μl 3 M $KHCO_3$/3.6 M KOH. Phenol red (0.4 μl of 0.2 mg/ml) was added as indicator. The sample was acidified with 1.14 μl of 1.8 M ammonium dihydrogen phosphate (pH 5.1) and 2.64 μl phosphoric acid (30%). Finally, the sample was centrifuged at 12,000 × g for 5 min and the supernatant was transferred to a new tube and stored at −20 °C. The supernatant was transferred to a new tube for HPLC analysis as described previously [24]. Adenosine content was normalized to volume. Adenosine concentration in T cell culture supernatant also was measured as above.

2.15. Statistical analysis

All results were expressed as means ± SEM of three independent experiments with each experiment including triplicate sets in vitro, or of eight animals per group in vivo. Student's *t* test was used to test the difference between two groups. One-way ANOVA and post hoc tests were applied when there were more than two groups in the independent variable. Kruskal-Wallis test was used for clinical score, X-ray score, histological score and immunohistochemical score assay. $P < 0.05$ was considered to be significant.

3. Result

3.1. Astilbin and low-dose MTX combination therapy alleviate the symptoms of CIA in DBA/1J mice, which is more effectively than alone group

All the DBA/1J mice were measured for the severity of arthritis by clinical score, incidence rate and body weight from day 28 to day 42. Compared with model group, astilbin and low-dose MTX combination therapy significantly alleviated the symptoms of CIA in clinic score, incidence rate and paw welling (Fig. 1A, B and D). Meanwhile, symptoms of bone erosion, articular destruction, joint displacement, synovial hyperplasia, inflammatory cell infiltration, angiogenesis in the inflamed synovium and destruction of cartilage, observed in CIA group, were reduced by combination therapy (Fig. 1E–J). Compared with single use, combination therapy showed better effect in most above indexes, without no extra side effect, even slightly improved the body change induced by low-dose MTX (Fig. 1A–J). Besides, expression of OB-cadherin, MCP-1, RANKL and MMP3 assayed by immunohistochemistry was consistent with the above symptoms (Fig. 2). Serum was harvested from all groups at the end of experiment at day 42. ELISA assay were used to determine the rheumatoid factors. Compared with model group, the levels of IgG, IgG1, IgG2a, IgG2b, IgM, were significantly decreased by combination therapy (Fig. 3A). Combination therapy showed better effect than single use in IgG, IgG1, IgG2a (Fig. 3A). Of note, we detected the anti-collagen IgG, and the results was in accordance with symptoms in clinical score (Fig. 3B). These data suggested the combination of astilbin and low-dose MTX was a more effective strategy to alleviate CIA than separate use.

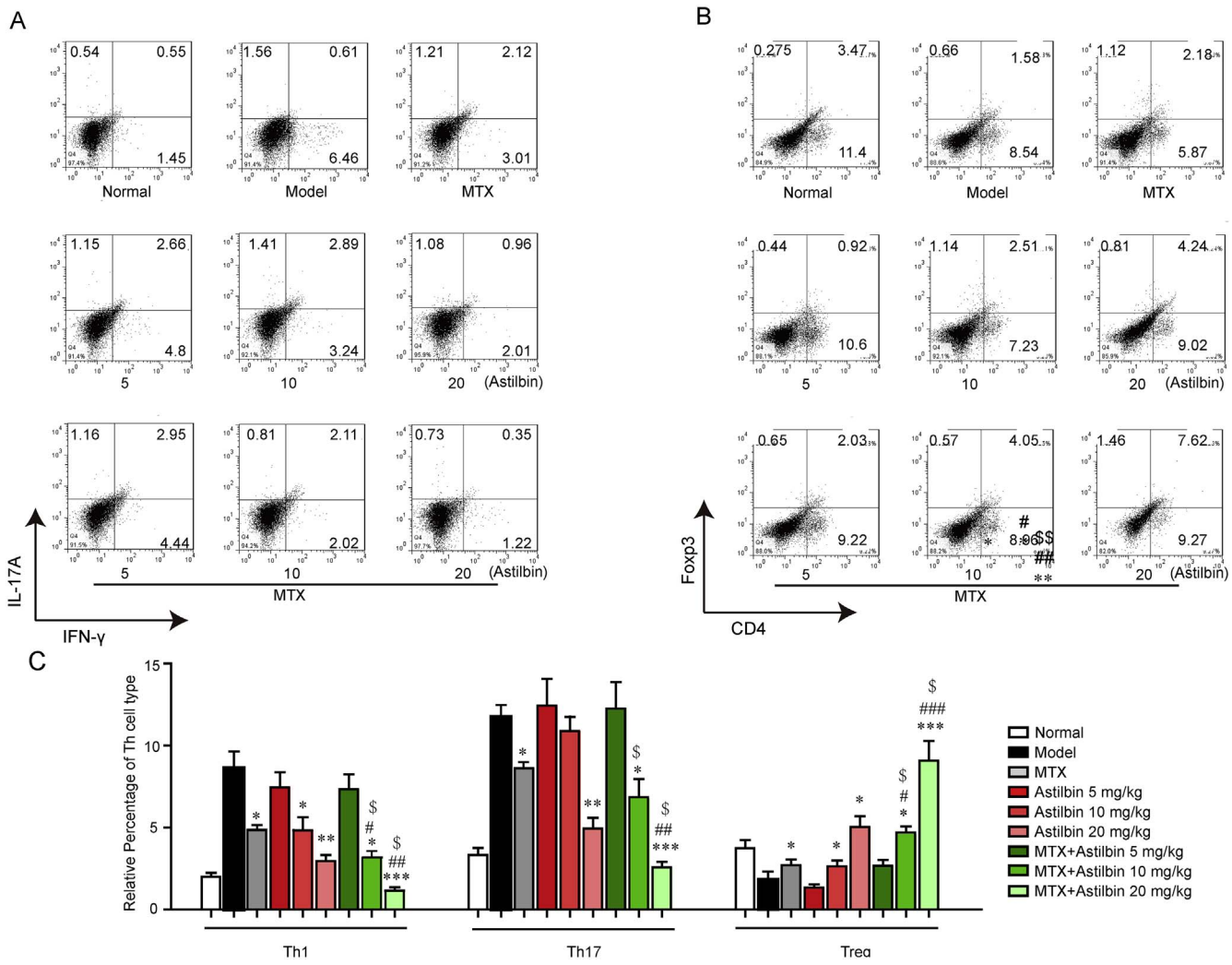

Fig. 5. Combination therapy regulates the balance of Th1/Th2 and Th17/Treg. Splenocytes isolated from DBA/1 mice on day 42 after immunization were cultured in RPMI 1640 containing 10% fetal calf serum with PMA/ionomycin containing monesin for 5 h. (A-C) Th1, TH17 and Treg cells were assessed by flow cytometer for $CD4^+IFN\text{-}\gamma^+$, $CD4^+IL17A^+$ and $CD4^+Foxp3^+$ cells. Representative data was shown here. Values are means ± SEM of each CIA group (n ≥ 8). $^*P \le 0.05$, $^{**}P \le 0.01$, $^{***}P \le 0.001$ versus model (black histogram). $^{\#}P \le 0.05$, $^{\#\#}P \le 0.01$ versus MTX alone (grey histogram). $^{\$}P \le 0.05$ versus corresponding astilbin alone (red histogram).

3.2. Combination therapy regulates the balance of Th1/Th2 and Th17/Treg

Pro-inflammatory cytokines, including IL-1β, IL-6, IFN-γ, TNF-α, IL-17A, were reduced, while the anti-inflammatory cytokine, IL-10, was obviously increased by combination treatment (Fig. 3B). Other cytokines were also tested, including IL-2 and IL-4. However, no significant changes were observed (Fig. 3B).

In order to confirm the results of serum, splenocytes were isolated from each group and activated with Con A for 48 h, then ELISA assay was used to detect the levels of supernatant cytokines related to the immune response. Similar result was observed that combination of astilbin and low-dose MTX showed more effective in IL-1β, IL-6, TNF-α, IFN-γ, IL-17A and IL-10 production than single use (Fig. 4A–H).

Flow cytometer was used to assess the percentage of $CD4^+IFN\text{-}\gamma^+$, $CD4^+IL17A^+$, $CD4^+Foxp3^+$ and $CD4^+IL4^+$ cells, which were isolated from lymph nodes of CIA mice and incubated with PMA/Ionomycine/Monensin for 5 h. Statistical results showed that astilbin inhibited Th1 and Th17 cell differentiation and enhanced Treg cell differentiation in dose-dependent manner, and the effects of combination groups were more remarkable under the dose of 20 mg/kg (Fig. 5A–C). However, the percent of Th2 cells almost had no change under astilbin, MTX or combination therapy (data not show).

3.3. Combination therapy strengthens single actions of astilbin or MTX in MAPK and inflammatory transcription factor pathways

To clarify the underlying mechanism of combination therapy with astilbin and MTX in RA, MAPK signals and transcription factors (NFκBp65, STAT1, STAT3 and STAT6) in T cells were examined. MTX at 0.1 μM slightly suppressed the Con A-induced activation of ERK1/2, JNK and P38, whereas astilbin significantly inhibited ERK1/2 activation (Fig. 6A and B). Combination group further dose-dependently reduced ERK1/2 activation, with no obvious effect in JNK and P38 activation (Fig. 6A and B). Besides, Con A-stimulated NFκBp65, STAT1 and STAT3 were mildly inhibited by MTX or astilbin alone, but the inhibitory action was enhanced by combination therapy (Fig. 6C and D). And, the anti-inflammatory transcription factor, STAT6, was up-regulated in MTX alone and combination groups, not astilbin groups (Fig. 6C and D).

3.4. MTX induces adenosine release, while astilbin increases $A_{2A}AR$ expression respectively

Adenosine has been shown to mediate the anti-inflammatory effect of MTX. Results from serum collected from every group of DBA/1J mice on the day 42 after immunization showed that MTX increased

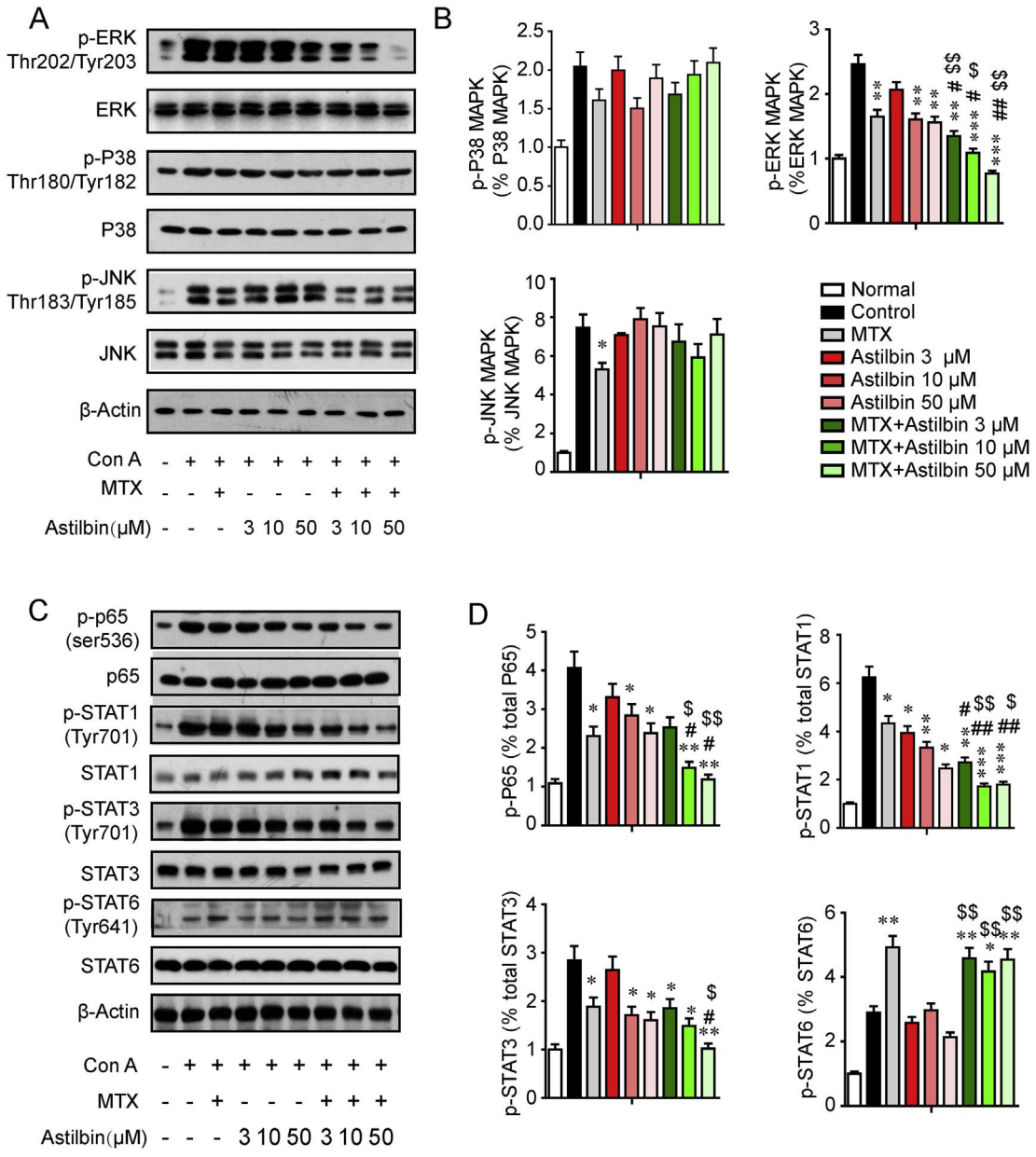

Fig. 6. Effects of combination therapy in MAPKs and inflammatory transcriptional factors pathways. T cells isolated from C57BL/6 mice were treated with indicated drugs for 1 h, and then stimulated by Con A (1 μM) for 24 h. Cell lysate was collected for western blot. MAPKs (A and B) and inflammatory transcriptional factors (C and D) were analyzed. Phospho-protein levels are expressed as means ± SEM normalized by corresponding total protein. $^{*}P \le 0.05$, $^{**}P \le 0.01$, $^{***}P \le 0.001$ versus control (black histogram). $^{\#}P \le 0.05$, $^{\#\#}P \le 0.01$ versus MTX (grey histogram). $^{\$}P \le 0.05$, $^{\$\$}P \le 0.01$, $^{\$\$\$}P \le 0.001$ versus corresponding astilbin alone (red histogram).

adenosine release, whereas astilbin did not (Fig. 7A and B). Moreover, to confirm the in vivo results, T cells from C57BL/6 mice were activated with Con A and treated with MTX, astilbin or combination. Then, the content of adenosine in T cells were determined. In accordance with serum result, in vitro test showed that MTX increased adenosine excretion but astilbin did not, and combination therapy showed no more increase on adenosine excretion (Fig. 7C).

We subsequently analyzed the expression of ARs. Interestingly, astilbin specifically increased the A_{2A}AR mRNA in T cells in a dose dependent manner without influence in other subtypes of ARs, whereas MTX even slightly decreased the expression of A_{2A}AR (Fig. 7D–G). This result was confirmed by WB analysis of A_{2A} AR in T cells (Fig. 7H and I).

3.5. Combination therapy mediates the anti-inflammation mainly through adenosine/A_{2A}AR/ERK axis

To further explore mechanism, T cells from C57BL/6 mice were activated with Con A and treated with different molecules as indicated in Fig. 8, and then cytokines were determined by ELISA and associated signals were analyzed by western blotting. Con A-stimulated pro-inflammatory cytokines, such as IFN-γ, IL-1β and TNF-α, were mildly inhibited by MTX, and the inhibitory effect was enhanced by combination with astilbin (Fig. 8A–C). IL-17A had the similar trend even though there was no significance (Fig. 8D). On the other hand, anti-inflammatory cytokine, IL-10, up-regulated by MTX, was enhanced by combination therapy (Fig. 8E). The additive effects of astilbin in combination were greatly blocked by ZM241385, a specific antagonist of A_{2A}AR (Fig. 8A–E). Meanwhile, ZM241385 also blocked the anti-inflammatory effects of astilbin and adenosine combination in Con A-

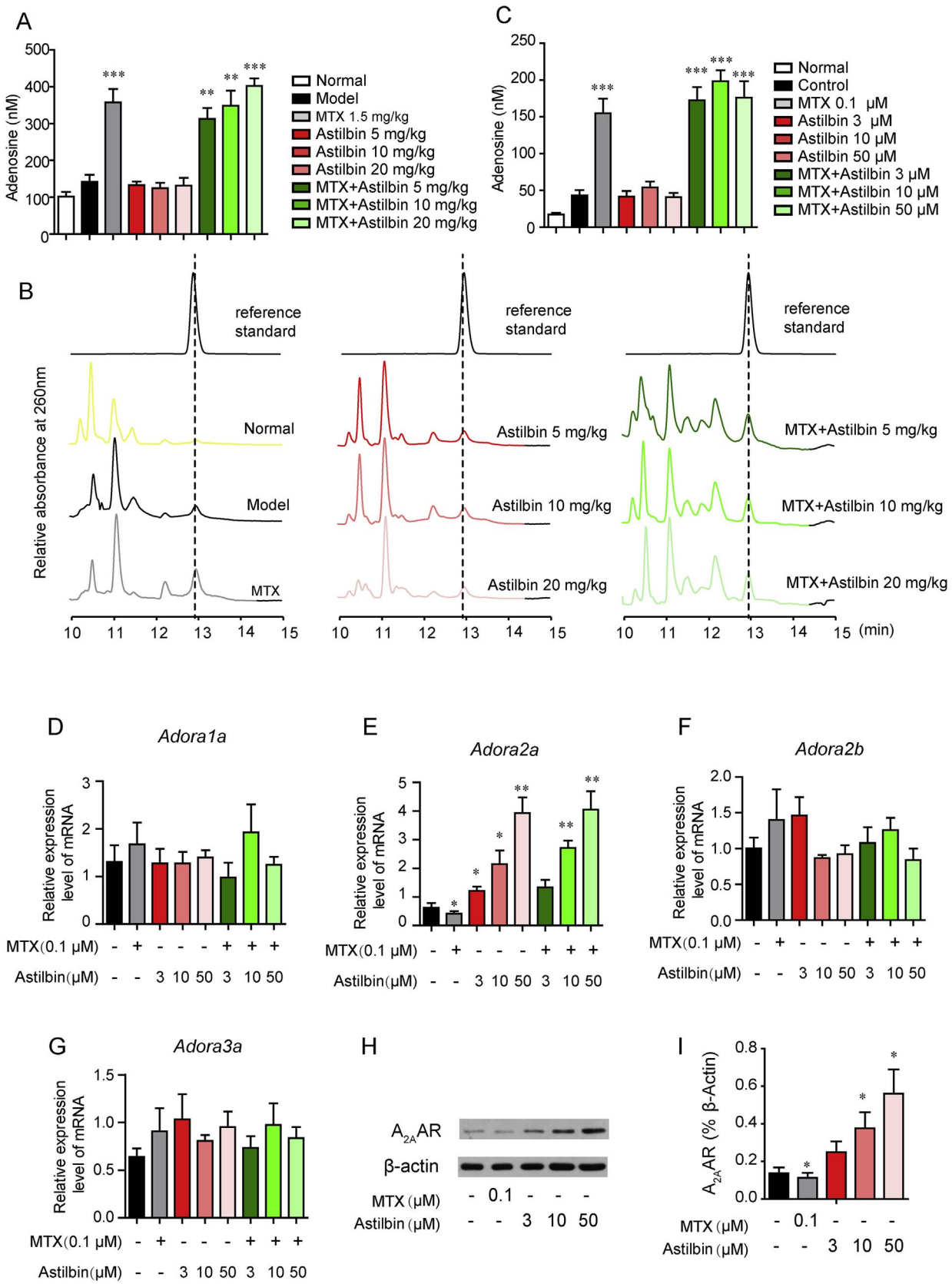

Fig. 7. MTX induces adenosine release, while astilbin increases A_{2A}AR expression respectively. Serum was collected as described in Fig. 3. (A and B) Adenosine levels of serum obtained from every group of DBA/1J mice on the day 42 post immunization was assessed by HPLC. (C-H) T cells isolated from C57BL/6 mice were pre-treated with indicated concentration of MTX or astilbin for 1 h, and then stimulated with Con A (1 μM) for 24 h. (C) Adenosine levels of T cells were assessed by HPLC. The mRNA levels of A_1R(D), $A_{2A}AR$(E), $A_{2B}AR$(F), $A_{3A}R$ (G) were analyzed by RT-PCR. (H-I) Protein levels of A_{2A}AR were examined by western blot. Values are means ± SEM of each treatment. $^{*}P \leq 0.05$, $^{**}P \leq 0.01$, $^{***}P \leq 0.001$ versus model (black histogram).

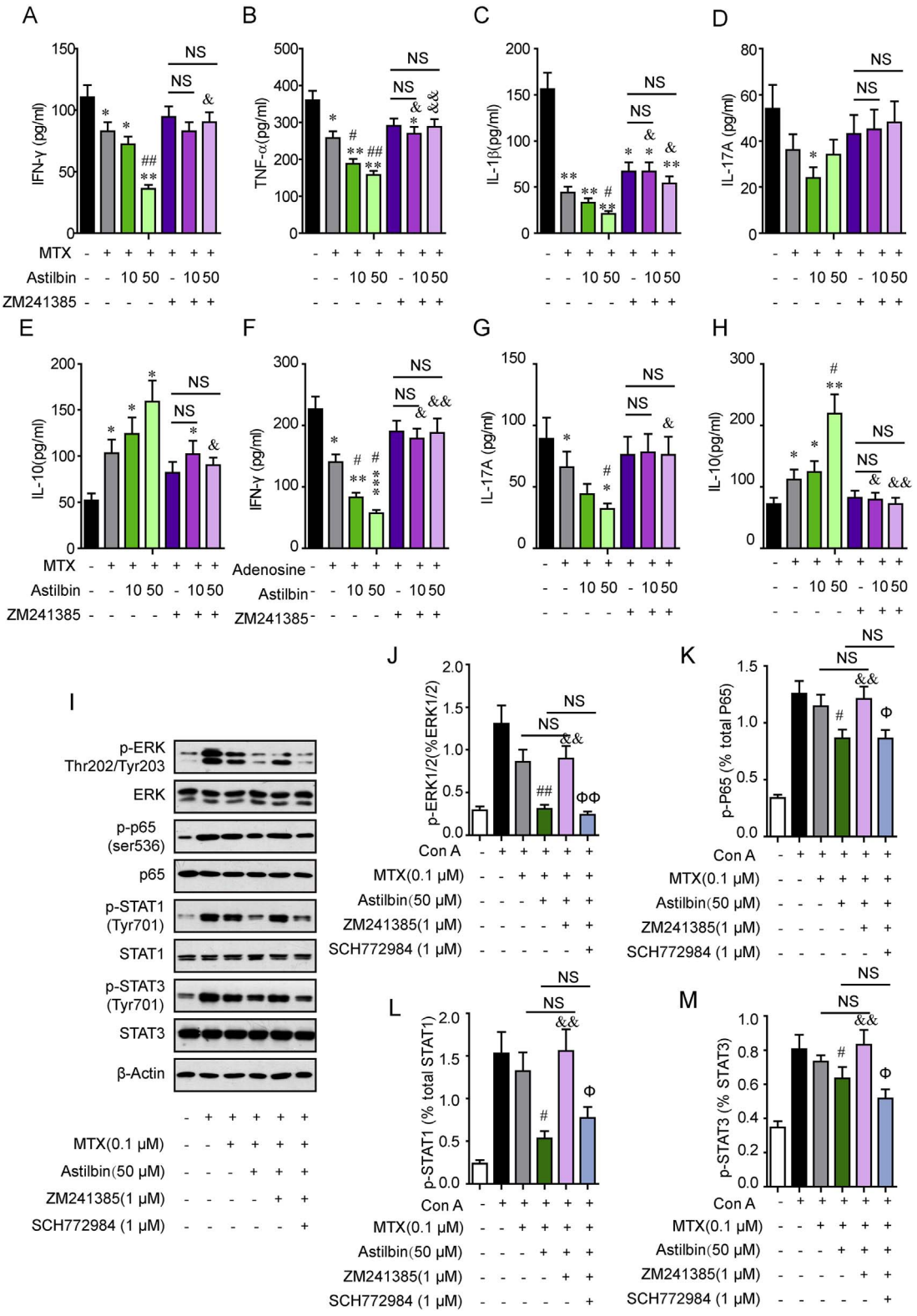

Fig. 8. ZM241385, specific antagonist of $A_{2A}AR$, blocked the additive effect of astilbin in combination with MTX in Con A-activated T cells. T cells isolated from C57BL/6 mice were treated with indicated drugs for 1 h, and then stimulated with Con A (1 μM) for 24 h. Supernatants and cells lysate were collected. (A–E) T cells treated with combination of MTX, astilbin and ZM241385 as shown. Levels of IFN-γ(A), TNF-α(B), IL-1β(C), IL-17A(D), IL-10(E) were analyzed by ELISA kits. (F-H) T cells treated with combination of MTX, adenosine and ZM241385 as mentioned above. Levels of IFN-γ (F), IL-17A (G), IL-10 (H) were analyzed by ELISA kits. Values are means ± SEM of each treatment. $^{*}P \le 0.05$, $^{**}P \le 0.01$, $^{***}P \le 0.001$ versus black histogram. $^{\#}P \le 0.05$, $^{\#\#}P \le 0.01$ versus grey histogram. $^{\&}P \le 0.05$, $^{\&\&}P \le 0.01$ versus green histogram. NS means no statistical significance. (I-M) T cells treated with MTX, astilbin, ZM241385 and SCH772984 as mentioned above. The levels of p-ERK1/2, p-P65, p-STAT1 and p-STAT3 were analyzed by western blot. Phospho-protein levels are expressed as means ± SEM normalized by corresponding total protein. $^{\#}P \le 0.05$ versus MTX alone (grey histogram). $^{\&}P \le 0.05$, $^{\&\&}P \le 0.01$ versus green histogram. $^{\Phi}P \le 0.05$, $^{\Phi\Phi}P \le 0.01$ versus pink histogram. NS means no statistical significance. The concentration of drugs was as follows: MTX (0.1 μM), adenosine (0.1 μM), SCH772984 (1 μM), ZM241385 (1 μM).

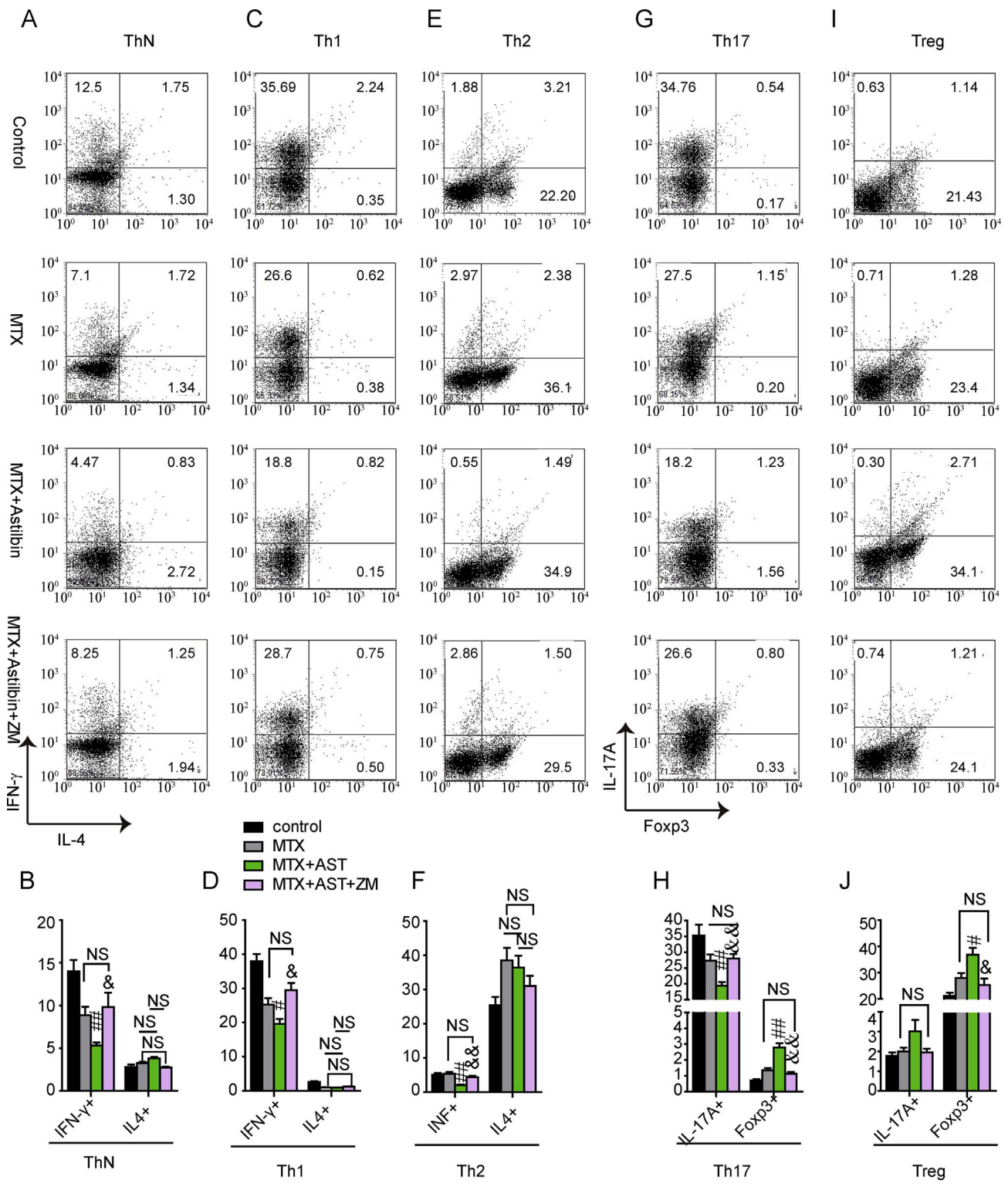

Fig. 9. ZM241385 blocked the function of combination therapy in balancing T cells differentiation. Naive CD4$^{\pm}$ T cells isolated from C57BL/6 mice were pre-treated with indicated drugs for 1 h, and then exposed to ThN, Th1, Th2, Th17 or Treg inducing conditions, as described in method. Frequency of IFN-γ-, IL-4- and IL-17-producing and Foxp3-expressing CD4^{+} T cells was analyzed by flow cytometer. Mean percentage of the indicated T-cell population ± SEM shown as histograms. (A and B) Frequency of IFN-γ- and IL-4-producing CD4^{+} T cells under ThN condition. (C and D) Frequency of IFN-γ- and IL-4-producing CD4^{+} T cells under Th1 condition. (E and F) Frequency of IFN-γ- and IL-4-producing CD4^{+} T cells under Th2 condition. (G and H) Frequency of IL-17A-producing and Foxp3-expressing CD4^{+} T cells under Th17 condition. (I and J) Frequency of IL-17A-producing and Foxp3-expressing CD4^{+} T cells under Treg condition. $^{\#}P \le 0.05$, $^{\#\#}P \le 0.01$ versus MTX (grey histogram). $^{\&}P \le 0.05$, $^{\&\&}P \le 0.01$ versus MTX + Astilbin (green histogram). AST and ZM stands for astilbin and ZM241385, respectively. The concentration of drugs was as follows: MTX (0.1 μM), astilbin (50 μM) and ZM241385 (1 μM).

activated T cells (Fig. 8F–H). Results of western blots showed that the inhibition of combination therapy on ERK1/2, NFκBp65, STAT1 and STAT3 was prevented by ZM241385 (Fig. 8I–M). SCH772984, a specific ERK1/2 inhibitor, reversed the effect of ZM241385 on NFκBp65, STAT1 and STAT3 (Fig. 8I–M).

3.6. Astilbin-mediated $A_{2A}AR$ upregulation contributed to balancing differentiation of T cells

Results showed that combo treatment of astilbin and MTX reduced the percentage of IFN-γ-producing Th1 cells under ThN/Th1/Th2 conditions, which was significantly blocked by ZM241385 (Fig. 9A–F). The percentage of IL-4-producing Th2 cells was not changed (Fig. 9A–F), suggesting that astilbin regulated Th1 and Th2 balance mainly by down-regulating Th1 cells. As well, under Th17-stimulating conditions, combination therapy decreased the IL-17A-producing Th17 cells and increased Foxp3-expressing Treg cells, which were reversed by ZM241385 (Fig. 9G and H). Under Treg-stimulating conditions, the percentage of inducible Treg cells was increased by combination treatment and ZM241385 prevented the effect (Fig. 9I and J).

4. Discussion

RA is a chronic aggressive autoimmune disease characterized by lesions of synovitis, bone damage and perpetuated inflammation in multiple joints [25]. Drug therapy for RA has evolved from salicylates, to NSAIDs, CSs, DMARDs, MTX, and finally to biologic response modifiers. MTX has become the initial drug of choice in most patients with RA. However, due to the side effects, some patients are unable to tolerate enough doses of MTX to achieve a clinical benefit [26]. Thus, low-dose of MTX combination therapy is an increasingly common use in clinic. In fact, leflunomide (LEF), ciclosporin (CSA), sulfasalazine (SSZ), intramuscular gold (IM gold) and anti-TNFα biologics have been used in MTX combined therapies in clinical [27,28]. However, these combinations increased the risk of side effects, compared with monotherapies [27]. For example, azathioprine [29] or IM gold [30] with MTX combinations increased the number of total side effects. Sulfasalazine [31–33] and leflunomide [34] in MTX combinations increased the risk of gastrointestinal (GI) side effects. Beside, leflunomide with MTX combination increased the risk of an abnormal liver function [34]. Therefore, discovery of new combination medicines with a novel mechanism to increase synergy and decrease toxic effects is necessary. We focused on the studies of astilbin for many years, and it exhibited anti-inflammatory and liver protective effects. [9,10]. In the present study, we identified that a co-therapeutic strategy with astilbin and low-dose MTX would be clinically desirable. Our results demonstrated that combined therapy of astilbin and low-dose MTX was more effective than monotherapies in reduction of disease activity (Figs. 1 and 2), and lower toxicity in liver injury, spleen and thymus index (data not show), which was extraordinarily different with other MTX-combined medicines and indicated desirable use in clinic.

Evidence showed that T cells differentiation may occur within the synovial membrane as a result of a favorable cytokine environment characterized by the presence of IL-1β, IL-6, TNF-α, IL-4, IL-17, IL-23, IL-10, TGF-β, et al. [35]. The pathogenesis of RA was viewed as the disregulation of Th1/Th2 or Th17/Treg balance, and the key players in this paradigm were the pro-inflammatory cytokine TNF-α and IFN-γ, which produced by Th1 cells [35]. IL-10 in combination with TGF-β can promote the differentiation of naive T cells to Treg cells, which in turn exert a nonspecific immunosuppressive effect that can inhibit Th17 and Th1 cells [36]. Our observations demonstrates that astilbin recovers the balance of Th1/Th2 and Th17/Treg by up-regulating Treg and down-regulating Th1 and Th17, which contributes to synergy in MTX-combination therapy (Figs. 1, 5 and 9). Besides, MTX alone at 1.5 mg/kg showed moderate effect in inflammatory cytokines and T cell differentiation, which were in accordance with clinical data [16]. Taken together, astilbin plays a better complementary role in low-dose MTX combination.

It is reported that the anti-inflammatory effect of MTX is due to adenosine release, which is known to exert potent anti-inflammatory effect [37,38]. Our findings confirmed that MTX increased adenosine release in vivo and in vitro (Fig. 7A–C), and astilbin up-regulated $A_{2A}AR$ expression (Fig. 7D–I). ZM241385, specific antagonist of $A_{2A}AR$, greatly blocked effects of astilbin and MTX combination on inflammatory cytokines and T cell differentiation (Figs. 8 and 9). Meanwhile, adenosine was used to mimic the action of MTX and examined the effect of astilbin. Similar results were achieved that astilbin strengthened the effect of adenosine on cytokines and this synergistic effect was block by ZM241385 (Fig. 8F–H). Accordingly, we provided a novel mechanism for drug combination in RA treatment that astilbin-mediated $A_{2A}AR$ overexpression enhanced the action of MTX-stimulated adenosine. Astilbin and MTX act on different aspect of adenosine signals and complement each other. This ligand and receptor system greatly contributes to the synergistic effect of astilbin and MTX combination therapy, which may be more effective than other MTX combination medicine.

Although $A_{2A}AR$ signals involving in T cell differentiation has been verified, particular signal transduction from $A_{2A}AR$ to inflammatory cytokines expression is still not clear [39,40]. MAPKs, NFκB and STATs are the downstream signals of $A_{2A}AR$ [41–44]. Our results indicated that ERK1/2, NFκB, STAT1 and STAT3 were involved in astilbin and MTX combination therapy (Fig. 6). And what's more, SCH772984, ERK1/2 inhibitor, could prevent the effect of ZM241385 on NFκB, STAT1 and STAT3 (Fig. 8I-M), indicating that ERK1/2 was the connecting point for $A_{2A}AR$ and inflammatory transcriptional factors.

In summary, combination therapy of astilbin and low-dose MTX ameliorated all symptoms of RA in CIA mice, decreased serum autoantibodies and pro-inflammatory cytokines and regulated Th1/Th17/Treg cell differentiation. In combination therapy, astilbin exerted its anti-inflammatory effect via enhancing expression of $A_{2A}AR$, and MTX simultaneously increased adenosine release, which augmented the synergistic effects. In addition, there were not obviously toxic effects of astilbin. Thus, the combination therapy of astilbin and low-dose MTX may be an effective strategy to control RA disease symptoms.

Conflict

The authors declare that they have no conflicts of interest concerning this article.

Acknowledgements

This work was supported by National Natural Science Foundation of China (Nos. 81473221, 81330079, 81673487, 21472091), Natural Science Foundation of Jiangsu Province (BK20161399) and the Fundamental Research Funds for the Central Universities (020814380076).

Author contribution

Study conception and design: X. Wu and Q. Xu; acquisition, analysis and/or interpretation of data: Y Ma, Z Gao, F. Xu, L Liu, Qiong Luo, Yan Shen, Xuefeng Wu, Xingxin Wu, Yang Sun; final approval and overall responsibility for the published work: X. Wu and Q. Xu.

References

[1] D.L. Scott, F. Wolfe, T.W. Huizinga, Rheumatoid arthritis, Lancet 376 (2010) 1094–1108.
[2] B. Combe, R. Landewe, C. Lukas, H.D. Bolosiu, F. Breedveld, M. Dougados, et al., EULAR recommendations for the management of early arthritis: report of a task force of the European Standing Committee for International Clinical Studies Including Therapeutics (ESCISIT), Ann. Rheumatic Dis. 66 (2007) 34–45.

[3] H.G. Evans, N.J. Gullick, S. Kelly, C. Pitzalis, G.M. Lord, B.W. Kirkham, et al., In vivo activated monocytes from the site of inflammation in humans specifically promote Th17 responses, Proc. Natl. Acad. Sci. U.S.A. 106 (2009) 6232–6237.
[4] K. Albrecht, K. Kruger, J. Wollenhaupt, R. Alten, M. Backhaus, C. Baerwald, et al., German guidelines for the sequential medical treatment of rheumatoid arthritis with traditional and biologic disease-modifying antirheumatic drugs, Rheumatol. Int. 34 (2014) 1–9.
[5] K.G. Saag, G.G. Teng, N.M. Patkar, J. Anuntiyo, C. Finney, J.R. Curtis, et al., American College of Rheumatology 2008 recommendations for the use of non-biologic and biologic disease-modifying antirheumatic drugs in rheumatoid arthritis, Arthrit. Rheumatism. 59 (2008) 762–784.
[6] C. Salliot, D. van der Heijde, Long-term safety of methotrexate monotherapy in patients with rheumatoid arthritis: a systematic literature research, Ann. Rheumatic Dis. 68 (2009) 1100–1104.
[7] E.H. Choy, C. Smith, C.J. Dore, D.L. Scott, A meta-analysis of the efficacy and toxicity of combining disease-modifying anti-rheumatic drugs in rheumatoid arthritis based on patient withdrawal, Rheumatol. (Oxford, England) 44 (2005) 1414–1421.
[8] R.N. Maini, F.C. Breedveld, J.R. Kalden, J.S. Smolen, D. Davis, J.D. Macfarlane, et al., Therapeutic efficacy of multiple intravenous infusions of anti-tumor necrosis factor alpha monoclonal antibody combined with low-dose weekly methotrexate in rheumatoid arthritis, Arthrit. Rheumatism. 41 (1998) 1552–1563.
[9] J. Wang, Y. Zhao, Q. Xu, Astilbin prevents concanavalin A-induced liver injury by reducing TNF-alpha production and T lymphocytes adhesion, J. Pharmacy Pharmacol. 56 (2004) 495–502.
[10] Y. Cai, T. Chen, Q. Xu, Astilbin suppresses collagen-induced arthritis via the dysfunction of lymphocytes, Inflamm. Res. 52 (2003) 334–340.
[11] M. Fei, X. Wu, Q. Xu, Astilbin inhibits contact hypersensitivity through negative cytokine regulation distinct from cyclosporin A, J. Allergy Clin. Immunol. 116 (2005) 1350–1356.
[12] R. Yan, Q. Xu, Astilbin selectively facilitates the apoptosis of interleukin-2-dependent phytohemagglutinin-activated Jurkat cells, Pharmacol. Res. 44 (2001) 135–139.
[13] H.W. Yi, X.M. Lu, F. Fang, J. Wang, Q. Xu, Astilbin inhibits the adhesion of T lymphocytes via decreasing TNF-alpha and its associated MMP-9 activity and CD44 expression, Int. Immunopharmacol. 8 (2008) 1467–1474.
[14] H. Huang, Z. Cheng, H. Shi, W. Xin, T.T. Wang, L.L. Yu, Isolation and characterization of two flavonoids, engeletin and astilbin, from the leaves of Engelhardia roxburghiana and their potential anti-inflammatory properties, J. Agric. Food Chem. 59 (2011) 4562–4569.
[15] L. Dong, J. Zhu, Astilbin from Smilax glabra Roxb. Attenuates inflammatory responses in complete freund's adjuvant-induced arthritis rats, eCAM 2017 (2017) 8246420.
[16] C. Lina, W. Conghua, L. Nan, Z. Ping, Combined treatment of etanercept and MTX reverses Th1/Th2, Th17/Treg imbalance in patients with rheumatoid arthritis, J. Clin. Immunol. 31 (2011) 596–605.
[17] X. Yu, C. Wang, J. Luo, X. Zhao, L. Wang, X. Li, Combination with methotrexate and cyclophosphamide attenuated maturation of dendritic cells: inducing Treg skewing and Th17 suppression in vivo, Clin. Develop. Immunol. 2013 (2013) 238035.
[18] B.N. Cronstein, Low-dose methotrexate: a mainstay in the treatment of rheumatoid arthritis, Pharmacol. Rev. 57 (2005) 163–172.
[19] G. Hasko, B.N. Cronstein, Adenosine: an endogenous regulator of innate immunity, Trends Immunol. 25 (2004) 33–39.
[20] B.B. Fredholm, I.J. AP, K.A. Jacobson, K.N. Klotz, J. Linden, International Union of Pharmacology. XXV. Nomenclature and classification of adenosine receptors, Pharmacol. Rev. 53 (2001) 527–552.
[21] T. Chen, J. Li, J. Cao, Q. Xu, K. Komatsu, T. Namba, A new flavanone isolated from rhizoma smilacis glabrae and the structural requirements of its derivatives for preventing immunological hepatocyte damage, Planta Medica. 65 (1999) 56–59.
[22] Q. Luo, Y. Sun, W. Liu, C. Qian, B. Jin, F. Tao, et al., A novel disease-modifying antirheumatic drug, iguratimod, ameliorates murine arthritis by blocking IL-17 signaling, distinct from methotrexate and leflunomide, J. Immunol. 191 (2013) 4969–4978.
[23] Y. Lee, A. Awasthi, N. Yosef, F.J. Quintana, S. Xiao, A. Peters, et al., Induction and molecular signature of pathogenic TH17 cells, Nat. Immunol. 13 (2012) 991–999.
[24] T.B.W.R. Knudsen, S.K. Otey, M.R. Blackburn, M.J. Airhart, J.K. Church, R.G. Skalko, Effects of (R)-deoxycoformycin (pentostatin) on intrauterine nucleoside catabolism and embryo viability in the pregnant mouse, Teratology (1992).
[25] I.B. McInnes, G. Schett, Cytokines in the pathogenesis of rheumatoid arthritis, Nat. Rev. Immunol. 7 (2007) 429–442.
[26] K.S. Upchurch, J. Kay, Evolution of treatment for rheumatoid arthritis, Rheumatology (Oxford, England) 51 (Suppl 6) (2012) vi28-36.
[27] W. Katchamart, J. Trudeau, V. Phumethum, C. Bombardier, Efficacy and toxicity of methotrexate (MTX) monotherapy versus MTX combination therapy with non-biological disease-modifying antirheumatic drugs in rheumatoid arthritis: a systematic review and meta-analysis, Ann. Rheumatic Dis. 68 (2009) 1105–1112.
[28] K. Albrecht, U. Muller-Ladner, Side effects and management of side effects of methotrexate in rheumatoid arthritis, Clin. Exp. Rheumatol. 28 (2010) S95–S101.
[29] R.F. Willkens, J.T. Sharp, D. Stablein, C. Marks, R. Wortmann, Comparison of azathioprine, methotrexate, and the combination of the two in the treatment of rheumatoid arthritis. A forty-eight-week controlled clinical trial with radiologic outcome assessment, Arthrit. Rheumatism. 38 (1995) 1799–1806.
[30] A.J. Lehman, J.M. Esdaile, A.V. Klinkhoff, E. Grant, A. Fitzgerald, J. Canvin, A 48-week, randomized, double-blind, double-observer, placebo-controlled multicenter trial of combination methotrexate and intramuscular gold therapy in rheumatoid arthritis: results of the METGO study, Arthrit. Rheumatism. 52 (2005) 1360–1370.
[31] M. Dougados, B. Combe, A. Cantagrel, P. Goupille, P. Olive, M. Schattenkirchner, et al., Combination therapy in early rheumatoid arthritis: a randomised, controlled, double blind 52 week clinical trial of sulphasalazine and methotrexate compared with the single components, Ann. Rheumatic Dis. 58 (1999) 220–225.
[32] C.J. Haagsma, P.L. van Riel, D.J. de Rooij, T.B. Vree, F.J. Russel, M.A. van't Hof, et al., Combination of methotrexate and sulphasalazine vs methotrexate alone: a randomized open clinical trial in rheumatoid arthritis patients resistant to sulphasalazine therapy, British J. Rheumatol. 33 (1994) 1049–1055.
[33] C.J. Haagsma, P.L. van Riel, A.J. de Jong, L.B. van de Putte, Combination of sulphasalazine and methotrexate versus the single components in early rheumatoid arthritis: a randomized, controlled, double-blind, 52 week clinical trial, British J. Rheumatol. 36 (1997) 1082–1088.
[34] J.M. Kremer, M.C. Genovese, G.W. Cannon, J.R. Caldwell, J.J. Cush, D.E. Furst, et al., Concomitant leflunomide therapy in patients with active rheumatoid arthritis despite stable doses of methotrexate. A randomized, double-blind, placebo-controlled trial, Ann. Internal Med. 137 (2002) 726–733.
[35] T. Kobezda, S. Ghassemi-Nejad, K. Mikecz, T.T. Glant, Z. Szekanecz, Of mice and men: how animal models advance our understanding of T-cell function in RA, Nat. Rev. Rheumatol. 10 (2014) 160–170.
[36] M.C. Boissier, E. Assier, G. Falgarone, N. Bessis, Shifting the imbalance from Th1/Th2 to Th17/treg: the changing rheumatoid arthritis paradigm, Joint, Bone, Spine: Revue du Rhumatisme 75 (2008) 373–375.
[37] N.P. Riksen, P. Barrera, P.H. van den Broek, P.L. van Riel, P. Smits, G.A. Rongen, Methotrexate modulates the kinetics of adenosine in humans in vivo, Ann. Rheumatic Dis. 65 (2006) 465–470.
[38] M.C. Montesinos, M. Takedachi, L.F. Thompson, T.F. Wilder, P. Fernandez, B.N. Cronstein, The antiinflammatory mechanism of methotrexate depends on extracellular conversion of adenine nucleotides to adenosine by ecto-5'-nucleotidase: findings in a study of ecto-5'-nucleotidase gene-deficient mice, Arthrit. Rheumatism. 56 (2007) 1440–1445.
[39] P.E. Zarek, C.T. Huang, E.R. Lutz, J. Kowalski, M.R. Horton, J. Linden, et al., A2A receptor signaling promotes peripheral tolerance by inducing T-cell anergy and the generation of adaptive regulatory T cells, Blood 111 (2008) 251–259.
[40] H. Eini, V. Frishman, R. Yulzari, L. Kachko, E.C. Lewis, C. Chaimovitz, et al., Caffeine promotes anti-tumor immune response during tumor initiation: involvement of the adenosine A2A receptor, Biochem. Pharmacol. 98 (2015) 110–118.
[41] S. Save, K. Persson, Effects of adenosine A(2A) and A(2B) receptor activation on signaling pathways and cytokine production in human uroepithelial cells, Pharmacology 86 (2010) 129–137.
[42] M.A. Ansari, A. Nadeem, S.M. Attia, S.A. Bakheet, M. Raish, S.F. Ahmad, Adenosine A2A receptor modulates neuroimmune function through Th17/retinoid-related orphan receptor gamma t (RORgammat) signaling in a BTBR T+ Itpr3tf/J mouse model of autism, Cell. Sign. 36 (2017) 14–24.
[43] A. Mediero, M. Perez-Aso, B.N. Cronstein, Activation of adenosine A(2A) receptor reduces osteoclast formation via PKA- and ERK1/2-mediated suppression of NFkappaB nuclear translocation, British J. Pharmacol. 169 (2013) 1372–1388.
[44] M.S. Giambelluca, M. Pouliot, Early tyrosine phosphorylation events following adenosine A2A receptor in human neutrophils: identification of regulated pathways, J. Leukocyte Biol. 102 (2017) 829–836.